MALAYSIAN JOURNAL OF ANALYTICAL SCIENCES

Journal homepage: https://mjas.analis.com.my/

Research Article

Optimising dazomet fungicide loading in calcium-based metal-organic frameworks: A solvent screening approach using high-performance liquid chromatography

Nurul Farhana Ahmad Aljafree[1,2], Umar Abd Aziz[1], Mohamad Firdaus Ahmad[3], Adila Jaafar[4], Norhayu Asib[3], and Mohd Basyaruddin Abdul Rahman[1,2*]

[1]Foundry of Reticular Materials for Sustainability, Institute of Nanoscience and Nanotechnology
[2]Department of Chemistry, Faculty of Science, Universiti Putra Malaysia, 43400 UPM Serdang, Selangor, Malaysia
[3]Department of Plant Protection, Faculty of Agriculture, Universiti Putra Malaysia, 43400 UPM Serdang, Selangor, Malaysia
[4]Centre of Foundation Studies for Agricultural Science, Universiti Putra Malaysia, 43400 UPM Serdang, Selangor, Malaysia

[*]Corresponding author: basya@upm.edu.my

Received: 12 February 2025; Revised: 11 June 2025; Accepted: 18 June 2025; Published: 22 August 2025

Abstract

Fungicides are essential for plants to combat plant pathogens that cause severe diseases, leading to significant yield losses and quality deterioration. Since the majority of fungicide active ingredients are unstable, inert additives like organic solvents must be used to create stable formulations for agrochemical products. To address this challenge, calcium L-lactate framework (MOF-1201) was synthesised using the solvothermal method. Powder X-ray diffraction confirmed that the framework exhibited a pattern similar to the simulated MOF-1201. The field emission scanning electron microscopy image showed that MOF-1201 displayed a rod-like morphology with a size range between 60.1 and 72.1 µm. In addition, MOF-1201 exhibited high thermal stability up to 400 °C. The encapsulation efficiency (EE) and loading capacity (LC) of the dazomet fungicide with different solvent concentrations were determined using high-performance liquid chromatography. The highest EE and LC values of dazomet were observed when ethanol was used as the solvent. MOF-1201 retained its crystallinity even after the incorporation of dazomet in its framework. In conclusion, the loading of dazomet fungicide strongly depends on solvent properties, highlighting the importance of solvent selection in optimising fungicide delivery systems.

Keywords: MOF-1201, stability, encapsulation, crystallinity, fungicide

Introduction

The increasing demand for sustainable and effective agricultural practices has prompted the development of advanced delivery systems for agrochemicals, particularly fungicides [1]. Calcium-based metal-organic frameworks (Ca-MOFs) have emerged as viable alternatives for the controlled release of active ingredients owing to their high surface area, tunable porosity, and biocompatibility [2]. Dazomet, a broad-spectrum fungicide effective against soil-borne pathogens, faces significant limitations due to its rapid degradation in the environment and poor solubility, which reduce its overall efficacy in controlling infections [3]. Incorporating dazomet into Ca-MOFs offers a potential solution to these challenges by improving its stability and enabling controlled release. However, the loading efficiency of dazomet in Ca-MOFs is influenced by the choice of solvent, which governs the interaction between the fungicide and the Ca-MOF structure.

The choice of solvent is a key factor influencing the loading efficiency of agrochemicals into MOFs, as it can significantly affect the interaction between the host framework and the guest molecule [4]. Solvent properties, such as polarity, solubility, and molecular size, are crucial for determining the amount of encapsulation and the stability of the resulting composite [5]. Optimising solvent selection is essential for enhancing dazomet encapsulation in Ca-MOFs, as solvents govern the physicochemical interactions between the fungicide and the host framework. In addition, the structural and chemical compatibility between the fungicide and the MOF host

is critical for achieving high loading capacities and controlled release profiles. A thorough understanding of the molecular interactions, such as hydrogen bonding, π-π stacking, and electrostatic forces, between dazomet and the Ca-MOF can provide insights into the encapsulation mechanism.

High-performance liquid chromatography (HPLC) provides a reliable analytical method for determining loading efficiency and investigating the release kinetics of dazomet Ca-MOFs [6]. By systematically screening a range of solvents, this study aims to identify optimal conditions for maximising dazomet loading while maintaining the structural integrity of the Ca-MOF. This research contributes to the growing body of research on MOF-based agrochemical delivery systems and provides a methodological framework for solvent screening that can be extended to other active ingredients and MOF architectures. By addressing the challenges of fungicide loading and release, this study paves the way for the practical application of MOFs in agriculture, offering a promising alternative to conventional delivery methods.

Materials and Methods

Materials

Calcium acetate monohydrate ($Ca(CH_3CO_2)_2 \cdot H_2O$, 99%, Sigma-Aldrich), L-lactic acid ($C_3H_6O_3$, 98%, Merck), ethanol absolute (C_2H_5OH, 99.5%, Merck), dazomet ($C_5H_{10}N_2S_2$, Merck), dimethylformamide (DMF, 99.8%, Merck), isopropyl alcohol ($(CH_3)_2CH$ OH, 99.5%, Merck), and deionised water were used as received without further purification.

Synthesis of calcium L-lactate framework (MOF-1 201)

The preparation of MOF-1201 was modified from Yang et. al. [7]. Approximately 0.071 g (0.4 mmol) of calcium acetate monohydrate was weighed and dissolved in 7 mL of anhydrous ethanol. Then, 0.072 g (0.8 mmol) of L-lactic acid was added to the metal solution with continuous stirring and sonicated for 10 min. The solution was placed in an oven at 125 °C for 96 h. Colourless rod-shaped crystals were formed at the bottom of the vial. The sample was washed with anhydrous ethanol three times for three days. The sample was then activated in vacuum (100 mbar) using a vacuum oven at 80 °C to remove solvent mol ecules. The yield of the obtained sample was 40.2%.

Incorporation of dazomet fungicide in MOF-1201 (Dazo-MOF1201)

About 100 mg of MOF-1201 was weighed and mixed with 10 mL of dazomet solution using three different solvents, namely ethanol, DMF, and isopropyl alcohol, each at a concentration of 10.0 mg mL^{-1}. The solutions were placed in a microwave Teflon container and subjected to microwave irradiation at 100 °C with 100 W for 10 min [8]. After the reaction, the mixture was allowed to cool to room temperature. The resulting products were centrifuged three times at 2,500 rpm for 10 min to remove any unentrapped dazomet molecules.

Physicochemical characterisation of MOF-1201 and Dazo-MOF1201

The powder X-ray diffraction (PXRD) pattern was recorded using a Shidmadzu-600 diffractometer, covering a range of 3–40° with a Cu-Kα radiation source (λ = 1.5405 Å) operated at 40 kV and 30 mA. Simulated PXRD patterns were obtained using the Mercury programme based on single crystal data [9]. Thermogravimetric analysis (TGA) was conducted at a heating rate of 10 °C min^{-1} from 50 to 800 °C and a nitrogen flow rate of 50 mL min^{-1}. The Fourier transform infrared (FTIR) spectroscopy analysis was conducted using a Shimadzu IRTracer-100 with a wavenumber range between 4000 and 400 cm^{-1} and over 32 cumulative scans. Field emission scanning electron microscopy (FESEM) images were obtained using a JEOL JSM-6400 microscope at an emission voltage of 5 kV. The samples were dried at room temperature for 12 h under vacuum to remove excess solvents. Nitrogen sorption measurements were conducted at 77 K using a BELSORP mini apparatus (Microtrac-BEL).

Measurement of dazomet content in MOF-1201

A Dionex Ultimate 3000 HPLC instrument was used to determine the content of dazomet. The analysis was performed using a Luna C18 column (250 mm × 4.6 mm, 10 µm). The isocratic mobile phase consisted of a mixture of methanol/water (30:70, v/v) with a flow rate of 1.0 mL min^{-1}. The column temperature was set at 28 °C, and the sample injection volume was 20 µL. The chromatogram was detected at 280 nm using a UV detector [10].

The loading capacity (LC) and encapsulation efficiency (EE) were calculated using the following equations:

$$LC = (A - B)/C \quad (1)$$

$$EE = (A - B)/A \quad (2)$$

where A is the total amount of added dazomet, B is the free amount of dazomet, and C is the weight of MOF-1201.

Results and Discussion

Synthesis and characterisation of MOF-1201

MOF-1201 was synthesised using Ca^{2+} as the metal nodes and both lactate and acetate as linkers [7]. Lactate and acetate molecules formed bridges that

connected to the Ca^{2+} centres to form a framework. The obtained MOF-1201 was observed to be crystalline under a light microscope at 20× magnification. As shown in **Figure 1(a)**, MOF-1201 exhibited colourless, rod-shaped crystals. The crystallinity of MOF-1201 was assessed by comparing the experimental and simulated PXRD patterns [11].

Figure 1(b) shows that the synthesised MOF-1201 m atched well with the simulated PXRD patterns at each stage, namely as-synthesised, solvent exchange, and activated, respectively. Four significant peaks were observed at lower angles (2θ = 3.5, 5.0, 7.5, and 10. 1°) in the synthesised MOF-1201. Although several peak intensities in MOF-1201 differed slightly from their simulated patterns, this variation does not affect the crystal structures, as the lattice parameters, symmetry, and space group of each crystal are related to peak positions rather than peak intensities [12]. These variations in peak intensities may be attributed to the preferred orientation of the MOF-1201 crystallites or slight differences in phase composition arising from variations in synthetic conditions [13, 14]. The PXRD data indicate that MOF-120 exhibited high crystallinity at each stage.

The FESEM image (**Figure 2(a)**) indicates that MOF -1201 exhibits a rod-like morphology, with crystal dimensions of 72.1 µm (length) and 5.71 µm (diameter). The rod-like structure is attributed to the use of calcium metal as a precursor. This finding is consistent with several studies that have used calcium metal sources for the synthesis of Ca-based MOFs [16]. Rod-like particles are known for their unique phase behaviour, including the ability to form an inter mediate liquid-crystalline phase between the liquid and solid states, which may influence molecular diffusion and release dynamics [17]. Such features could make MOF-1201 advantageous for enhancing the loading of dazomet fungicide. The thermal decomposition pattern of MOF-1201 comprises three stages occurring at 155, 453, and 544 °C (**Figure 2 (b)**).

The first stage of thermal decomposition is associated with the decomposition of solvent molecules (9.5%), followed by the loss of coordinated hydroxy and acetate linkers (39.3%) in the second stage. The third stage is associated with the loss of coordinated carbo xyl linker (24.8%) and the total collapse of the MOF-1201 framework [7]. Nitrogen sorption measurements at 77 K were subsequently conducted for MOF-1201 (Figure 2(c)). The results indicated that MOF-1201 exhibited a fully reversible type I isotherm, indicating that it possesses permanent microporosity. The Brunauer-Emmett-Teller surface area of MOF-1201 was found to be 323.75 m^2/g.

Loading of dazomet fungicide in MOF-1201 (Dazo -MOF1201)

The calibration curves of dazomet (20, 40, 60, 80, and 100 µg mL^{-1}) were established using ethanol, DMF, and isopropyl alcohol as solvents. As shown in **Figure 3**, the coefficient of determination (R^2) values for the standard curve of dazomet were 0.998, 0.997, and 0.994 in ethanol, DMF, and isopropyl alcohol, respectively. According to **Table 1**, the EE% and LC% of dazomet in MOF-1201 varied significantly with the solvent used, with ethanol exhibiting the highest efficiency, followed by isopropyl alcohol and DMF. This variation can be attributed to differences in solvent properties, including polarity, molecular size, and evaporation rate [5]. In contrast, isopropyl alcohol, being less polar and slightly larger, demonstrated reduced solubility of dazomet, which could lead to lower EE [15]. Although DMF possesses high polarity and strong solvating power, its larger molecular structure and low evaporation rate hinder dazomet's access to the MOF pores, resulting in poor loading of dazomet in MOF-1201.

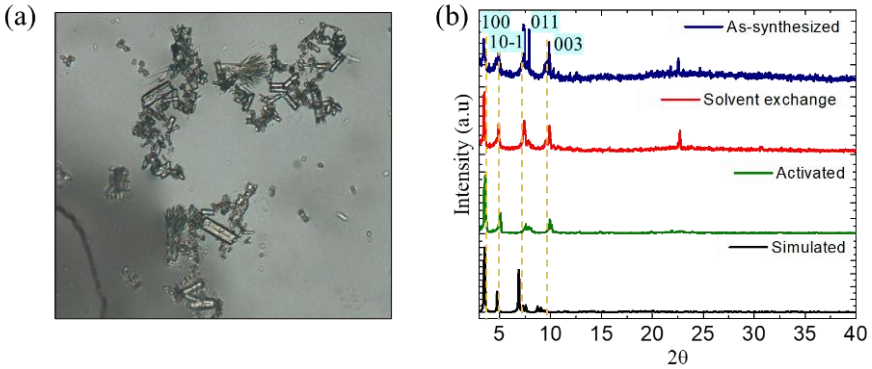

Figure 1. a) Structure of MOF-1201 observed under a light microscope at 20× magnification and b) PXRD patterns of experimental MOF-1201 (blue, red, and green) compared to the simulated MOF-1201 pattern (black)

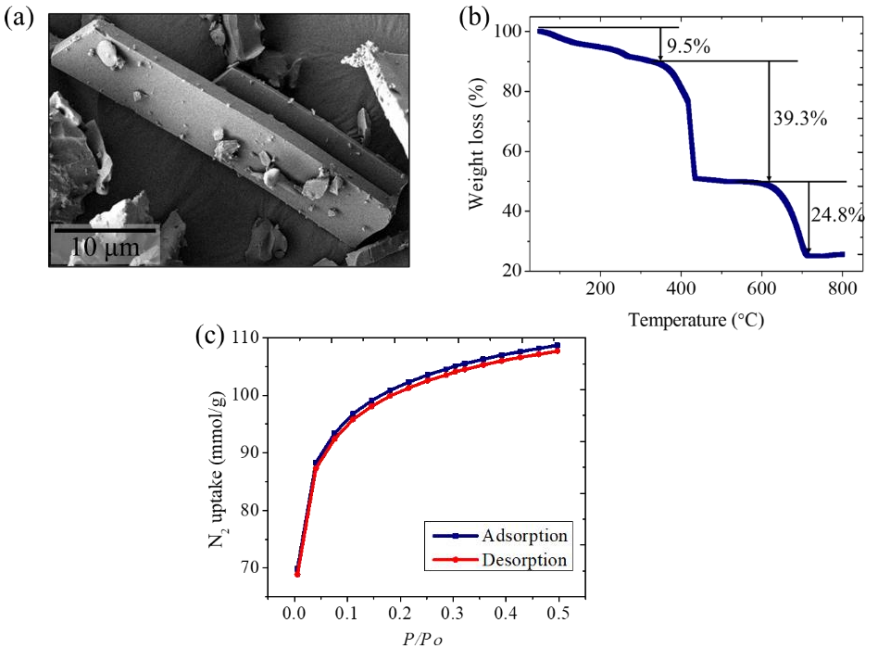

Figure 2. a) FESEM images of MOF-1201 at 1,000× magnification, b) TGA of MOF-1201, and c) nitrogen isotherm of MOF-1201

Additionally, the hydrogen bonding capability of the solvents plays a critical role in the loading of dazomet fungicide. Ethanol exhibits higher hydrogen bonding capacity compared to isopropyl alcohol due to its simpler molecular structure, which features only one alkyl group attached to the hydroxyl group, allow ing for more potential hydrogen bond interactions with neighbouring molecules, whereas isopropyl alcohol has a branched structure with two alkyl groups attached to the hydroxyl group, which hinders its ability to form as many hydrogen bonds [18]. How ever, DMF lacks strong hydrogen bonding ability because it does not have a readily available hydrogen atom directly bonded to a highly electronegative atom like oxygen, which is necessary for forming a hydrogen bond [19].

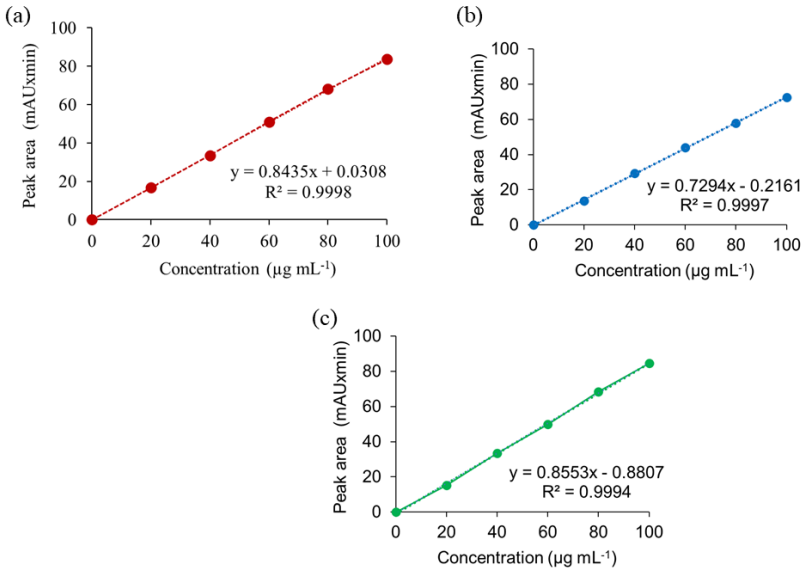

Figure 3. Calibration curves of dazomet in a) ethanol, b) DMF, and c) isopropyl alcohol

Table 1. Amount of dazomet loaded in MOF-1201 at different concentrations.

Type of Solvent	Encapsulation Efficiency (%)	Loading Capacity (%)
Ethanol	79.39 ± 0.7	0.79 ± 0.8
DMF	23.11 ± 0.5	0.23 ± 1.0
Isopropyl alcohol	42.65 ± 0.8	0.43 ± 0.9

Physicochemical characterisation of Dazo-MOF 1201

The PXRD patterns revealed the presence of both peaks at lower and higher angles of Dazo-MOF1201 (**Figure 4(a)**). The presence of lower angle peaks in Dazo-MOF1201 is similar to those of the pristine MOF-1201, suggesting that the crystallinity of MOF-1201 was retained after the encapsulation of dazomet in the framework. Furthermore, the presence of peaks at higher angles in Dazo-MOF1201 indicate d that dazomet was incorporated into the framework. The slight shifts observed in some peaks of Dazo-MOF1201 may be attributed to the deposition of some dazomet molecules on the surface of MOF-1201 [21]. **Figure 4(b)** shows the FTIR spectra of MOF-1201, dazomet, and Dazo-MOF1201. A broad O-H stretching at 3350 cm^{-1} was observed in Dazo-MOF 1201 compared to pristine MOF-1201 and dazomet. This broad O-H peak is correlated with strong hydrogen bonding between structural atoms, along with the additional N-H stretching [20]. In this case, the presence of the hydroxyl group from MOF-1201 and the amine group from dazomet enhanced the broadening of O-H peaks in Dazo-MOF1201. At 1750 cm^{-1}, a COO^- stretching peak was observed in both MOF-1201 and Dazo-MOF1201, corresponding to the presence of the carboxyl group from the linkers. The minor shifts in the COO^- band could indicate that the intermolecular interactions between Ca^{2+} and the linkers were weakened in the presence of dazomet molecules [21]. Several addition al peaks were seen in the fingerprint region of Dazo-MOF1201, indicating that dazomet was attached to the MOF-1201 framework.

Conclusion

In this study, MOF-1201 was successfully synthesise d and characterised. Pristine MOF-1201 possessed high crystallinity and thermally stable up to 400 °C. Furthermore, the loading of dazomet fungicide in MOF-1201 is highly dependent on the properties of the solvent. Significant variations were observed, with ethanol emerging as the optimal solvent due to its moderate polarity, small molecular size, and effective hydrogen bonding capability. These factors collectively facilitate efficient dazomet loading within MOF-1201. These findings underscore the importance of solvent selection in optimising dazomet loading in Ca-MOF, providing valuable insights for the development of advanced agrochemical delivery systems.

Acknowledgement

This work was supported by the Ministry of Energy, Science, Technology, Environment, and Climate Change (MESTECC-IF09180O1033). We would like to thank Prof. Omar Yaghi, Kyle E. Cordova, and Dr. Ha Lac Nguyen from the Department of Chemistry, University of California, Berkeley for their helpful in sights.

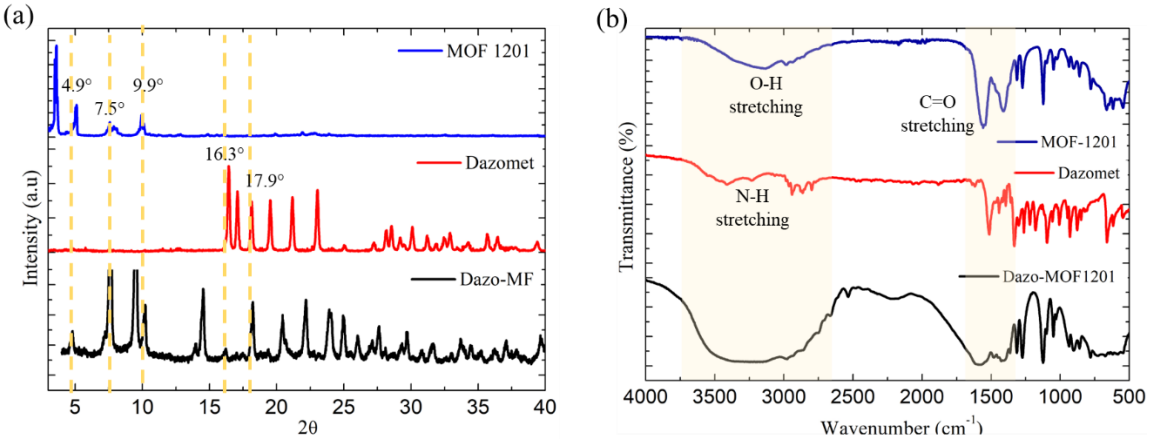

Figure 4. a) PXRD patterns and b) FTIR spectra of MOF-1201 (blue), dazomet (red), and Dazo-MOF1201 (black)

References

1. Ahmad, M. F., Ahmad, F. A., Alsayegh, A. A., Zeyaullah, M., AlShahrani, A. M., Muzammil, K., Saati, A. A., Wahab, S., Elbendary, E. Y., Kambal, N., Abdelrahman, M. H., and Hussain, S. (2024). Pesticides impacts on human health and the environment with their mechanisms of action and possible counter measures. *Heliyon,* 10(7): e29128.
2. Yusuf, V. F., Malek, N. I., and Kailasa, S. K. (2022). Review on metal–organic framework classification, synthetic approaches, and influencing factors: Applications in energy, drug delivery, and wastewater treatment. *ACS Omega*, 7(49): 44507-44531.
3. Lin, Y., Li, M., Dai, C., Liu, Y., Zhang, W., Yang, Q., Cui, X., and Yang, Y. (2024). Dazomet fumigation modification of the soil microorganism community and promotion of *Panax notoginseng* growth. *Frontiers in Microbiology*, 15: 1443526.
4. Pacheco, A., Attard, T., Calvert, D., Bullock, J., Clark, J. H., Sherwood, J., and McElroy, C. R. (2023). Green solvent selection for emulsifiable concentrate agrochemical formulations. *Organic Process Research & Development*, 28(1): 132-136.
5. Zhi, J., Huang, S., Zhu, X., Adra, H. J., Luo, K., and Kim, Y. (2023). Impact of solvent polarity on the morphology, physicochemical properties, and digestibility of A-type resistant starch particles. *Food Chemistry*, 418:135942.
6. Norton, A. E., Brabec, D. L., Tilley, M., Yeater, K. M., and Scheff, D. S. (2022). Quantification of methoprene aerosol deposition using reversed-phase high-performance liquid chromato graphy. *Journal of Stored Products Research*, 99: 102039.
7. Yang, J., Trickett, C. A., Alahmadi, S. B., Alshammari, A. S., and Yaghi, O. M. (2017). Calcium l-lactate frameworks as naturally degradable carriers for pesticides. *Journal of the American Chemical Society*, 139(24): 8118-8121.
8. Ranjbar, M., Pardakhty, A., Amanatfard, A., and Asadipour, A. (2018). Efficient drug delivery of β-estradiol encapsulated in Zn-metal–organic framework nanostructures by microwave-assisted coprecipitation method. *Drug Design, Development and Therapy,* 12: 2635-2643.
9. MacRae, C. F., Sovago, I., Cottrell, S. J., Galek, P. T. A., McCabe, P., Pidcock, E., … and Wood, P. A. (2020). Mercury 4.0: From visualization to analysis, design and prediction. *Journal of Applied Crystallography,* 53: 226-235.
10. Maluin, F. N., Hussein, M. Z., Yusof, N. A., Fakurazi, S., Seman, I. A., Hilmi, N. H. Z., and Daim, L. D. J. (2019). Enhanced fungicidal efficacy on *Ganoderma boninense* by simultaneous co-delivery of hexaconazole and dazomet from their chitosan nanoparticles. *RSC Advances*, *9*(46): 27083-27095.
11. Saini, K., Joseph, F., Ramanan, A., and Sharma Bhatia, S. (2017). Electrochemical synthesis of a oxalate-linked copper (II) metal organic frameworks: X-ray crystallographic structure and its magnetic properies. *Materials Today: Proceedings,* 4(9): 9616-9621.
12. Liu, K., Shen, Z. R., Li, Y., Han, S. De, Hu, T. L., Zhang, D. S., … and Ruan, W. J. (2014). Solvent induced rapid modulation of micro/nano structures of metal carboxylates coordination polymers: Mechanism and morphology dependent magnetism. *Scientific Reports,* 4: 1-7.
13. Molavi, H. and Salimi, M. S. (2025). Investigation the effect of exchange solvents on the adsorption performances of Ce-MOFs towards organic dyes. *Scientific Reports,* 15(1): 1-17.
14. Hurd, J. A., Vaidhyanathan, R., Thangadurai, V., Ratcliffe, C. I., Moudrakovski, I. L., and Shimizu, G. K. H. (2009). Anhydrous proton conduction at 150 °C in a crystalline metal–organic framework. *Nature Chemistry,* 1(9): 705-710.
15. Katritzky, A. R., Fara, D. C., Yang, H., Tämm, K., Tamm, T., and Karelson, M. (2004). Quantitative measures of solvent polarity. *Chemical Reviews*, 104(1): 175-198.
16. Thode, A. B., Kruse, S. W., Nix, J. C., and Jones, D. N. (2008). The role of multiple hydrogen-bonding groups in specific alcohol binding sites in proteins: Insights from structural studies of LUSH. *Journal of Molecular Biology*, 376(5): 1360-1376.
17. Wittmann, M., Henze, K., Yan, K., Sharma, V., and Simmchen, J. (2023). Rod-shaped microparticles — an overview of synthesis and properties. *Colloid and Polymer Science,* 301: 783-799
18. Naz, H., Ali, R. N., Premlatha, S., Liu, Y., and Zhu, G. (2024). Recent advances in hydrogen bonded organic frameworks and their derived materials for electrocatalytic water splitting. *Journal of Environmental Chemical Engineering*, 12(3): 112815.
19. Ben, A., Amaro-gahete, J., Esquivel, D., Romero-salguero, F. J., and Caballero, Á. (2020). MIL-88A metal-organic framework as a stable sulfur-host cathode for long-cycle Li-S batteries. *Nanomaterials,* 10(424): 1-14.
20. Hadjiivanov, K. I., Panayotov, D. A., Mihaylov, M. Y., Ivanova, E. Z., Chakarova, K. K., Andonova, S. M., and Drenchev, N. L. (2020). Power of infrared and raman spectroscopies to

characterize metal- organic frameworks and investigate their interaction with guest molecules. *Chemical Reviews,* 121(3): 1286-1424.

21. Dhumal, N. R., Singh, M. P., Anderson, J. A., Kiefer, J., and Kim, H. J. (2016). Molecular interactions of a Cu-Based Metal–Organic framework with a confined imidazolium-based ionic liquid: A combined density functional theory and experimental vibrational spectroscopy study. *The Journal of Physical Chemistry C,* 120(6): 3295-3304.